

DOI: 10.1070/QEL16254

Laser structuring of the diamond surface in the nanoablation regime

V.M. Gololobov, V.V. Kononenko, V.I. Konov

Abstract. **The possibility of using nanoablation (graphitisation-free photoinduced etching) for precise micro- and nanostructuring of the surface of a diamond single crystal has been experimentally investigated. The processing has been performed by femtosecond third-harmonic pulses of a Ti : sapphire laser (λ = 266 nm). The specific features of the formation of a surface nanorelief (regularity of the newly formed structures and reduced nanoablation rate near craters) are discussed. The possibility of fabricating a diamond phase diffraction grating with a relief depth of ~130 nm is demonstrated and the diffraction pattern recorded at λ = 532 nm is compared with the results of theoretical analysis.**

Keywords: *nanoablation, micro- and nanostructuring of surface, diamond single crystal.*

1. Introduction

The development of modern photonics calls for mastering and implementing new promising materials. An ideal candidate is diamond, which has unique physical properties [1, 2]. Due to the transparency in a wide spectral range and high thermal conductivity, diamond is successfully used as an optical material in high-power IR lasers [3]. In addition, diamond, which is characterised by elevated radiation resistance, is applied as a material of radiation detectors [4]. However, high hardness and chemical inertness of diamond limit its practical applications. A promising tool for micro- and nanostructuring of the diamond surface is laser irradiation.

The conventional method of laser processing of diamond is based on pulsed heating and evaporation (ablation) of the surface layer of the processed sample, which is accompanied by graphitisation: transformation of the diamond lattice into amorphous carbon phase in the irradiated region [5]. The thickness of this strongly absorbing layer depends on the laser pulse duration and reaches several micrometers for microsecond pulses [6]. Currently, the graphitised layer is removed using selective surface oxidation, which occurs in a relatively narrow temperature range (580–620 °C). However, neither this technique nor other methods (e.g., plasma-chemical etching) provide a complete removal of the radiation-modified carbon phase from the surface [7].

Laser graphitisation of diamond is an interesting and important phenomenon. The possibility of close coexistence of the conducting and nonconducting phases of diamond opens interesting prospects for some applications [8]. However, in optical applications, the occurrence of graphitisation is most often associated with undesirable loss due to absorption, which must be eliminated. This is especially important for elements of power optics, e.g., diamond diffraction elements, whose radiation resistance is determined by the presence of absorbing inclusions.

In this study, we analyse the possibility of using an alternative laser method – nanoablation [9] – to form a nanorelief of a diamond optical element. This process is based on photostimulated oxidation in the presence of atmospheric oxygen, which is a dominant mechanism of surface etching under irradiation with energy densities below the graphitisation threshold. Based on the analysis of the data on latent accumulation graphitisation, it was suggested in [10] that nanoablation is a two-stage process. The first stage, apparently, implies nanographitisation, when lattice bonds are transformed as a result of strong perturbation of the electron subsystem (the induced plasma density exceeds 10^{20} cm^{-3}). Then the modified graphite clusters on the surface are oxidised, having no enough time to reach a certain critical size and initiate ablation.

Indeed, the formation of the graphite-like phase in the regions exposed to laser irradiation in nanoablation regimes has not been observed to date. Nanoablation is a 'soft' treatment, which does not destroy the crystal structure. However, its drawback is relatively low removal rates of the material (less than an atomic layer per pulse [11, 12]).

Diamond nanoablation rates have been measured for many laser sources with different radiation wavelengths and pulse durations [11, 12]. The depths of the craters obtained in these experiments generally did not exceed 10–20 nm. The purpose of the experiments described below was to form a regular structure with a depth of about 150 nm and study its optical properties. At this depth of the structure, the spatial phase modulation in the beam light reflected from it reaches ~π rad, which in principle allows one to control the reflected beam.

2. Experimental

The experiments were performed using a laser system including a Tsunami Ti : sapphire laser (Spectra Physics) and a

V.M. Gololobov A.M. Prokhorov General Physics Institute, Russian Academy of Sciences, ul. Vavilova 38, 119991 Moscow, Russia; e-mail: viktor-gololobov@yandex.ru;
V.V. Kononenko, V.I. Konov A.M. Prokhorov General Physics Institute, Russian Academy of Sciences, ul. Vavilova 38, 119991 Moscow, Russia; National Research Nuclear University 'MEPhI', Kashirskoe sh. 31, 115409 Moscow, Russia;
e-mail: vitali.kononenko@gmail.com, vik@nsc.gpi.ru

Received 9 November 2016
Kvantovaya Elektronika **46** (12) 1154–1158 (2016)
Translated by Yu.P. Sin'kov

Spitfire regenerative amplifier (Spectra Physics). This system provided 100-fs pulses with a repetition rate of 1 kHz at a wavelength of 800 nm. Two nonlinear b-BaB_2O_4 (BBO) crystals were used to generate the third harmonic (λ = 226 nm). The object of study was a diamond single crystal, grown by plasma-enhanced chemical vapour deposition and mechanically polished to the optical quality.

The laser beam was focused by an aspherical quartz lens with a focal length of 30 mm onto the surface of a diamond crystal oriented in the [100] direction. To determine the intensity distribution in the laser spot at relatively high pulse energies in the evaporative ablation mode, a series of small craters was formed on the sample surface. The dependence of the sizes of these craters on energy was used to reconstruct the beam energy density profile, which was close to Gaussian with a radius of 2 μm (at the level of 1/e). The multipulse graphitisation threshold measured for the irradiation by 0.5×10^6 pulses under these focusing conditions was $\sim$0.5 J cm^{-2}. To guarantee the absence of graphitisation under long-term irradiation, the average energy density was chosen to be $\sim$0.4 J cm^{-2}.

The surface profile was studied by a New View 5000 interference profilometer (Zygo) with a measurement error less than 1 nm; this accuracy made it possible to observe nanoablation-induced changes in the sample surface topology in the irradiated spot.

3. Results

3.1. Regularity of diamond structuring under nanoablation conditions

When designing optical elements, the reproducibility of their relief structure is of key importance. Since the laser treatment of the surface results in the successive formation of individual structural blocks (craters in our case), the regularity is mainly determined by the etch rate stability. The latter, in turn, is affected by two factors: pulse-to-pulse variations in the radiation energy and the inhomogeneity of crystal surface structure from point to point.

The influence of fluctuations of individual pulse energy can be estimated from the relations between the etch rate and the energy density in the spot for a specific laser source.

Note that these relations are generally strongly nonlinear, because diamond is a wide-gap insulator, and the radiation energy is transferred to its lattice as a result of multiphoton absorption. This circumstance makes the requirements to the pulsed beam stability more stringent.

Concerning the variations in the crystal structure from point to point, this problem is more intricate. The details of the nanoablation mechanism (in particular, the role of the laser heating of crystal and the laser-induced ionisation) are not quite clear to date. Therefore, it is untimely to attribute etch rate fluctuations to specific lattice inhomogeneities. These may be either point defects in the oxidised layer of material (about 1000 atomic layers thick) or absorbing inclusions in the laser energy dissipation domain with a thickness of $\sim$1 μm (the two-photon absorption coefficient β = 0.9 cm GW^{-1} for λ = 266 nm [13]). The purpose of our experiments was to measure the point-to-point crater depth fluctuations on the surface and estimate the contribution of the inhomogeneities initially present in the crystal to these fluctuations.

Figure 1 shows the dynamics of change in the laser pulse energy and the corresponding depths of the craters formed under irradiation (3×10^6 pulses per crater). During the laser treatment the energy was measured ten times at each surface point (i.e., in the crater). The relative standard deviation of the laser beam energy during the treatment was $s_E \approx 1.5\%$. In the case of irradiation by femtosecond UV pulses with λ = 266 nm, the etch rate r depends on energy density F as $r \sim F^4$ [12]. Under these conditions, the crater depth fluctuations s_r should be larger by a factor of about 4: approximately 6%.

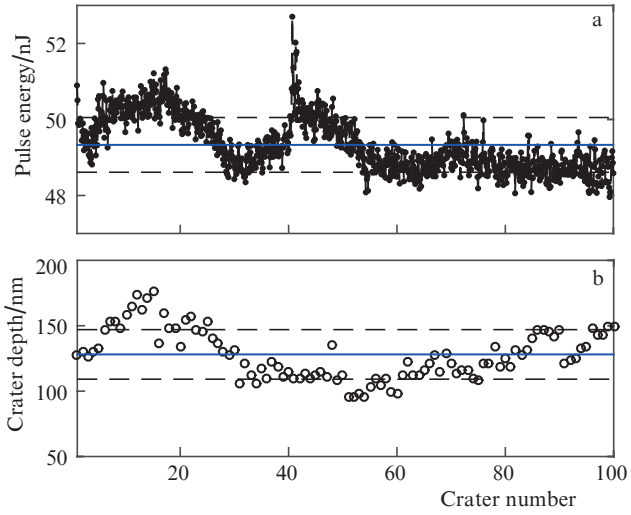

Figure 1. (a) Dynamics of changes in the laser energy and (b) the corresponding crater depths (3×10^6 pulses per crater).

However, the relative spread over depth turned out to be larger: $s_r \approx 15\%$, which can be explained by the aforementioned effect of the inhomogeneity of specific sample material. Note that Fig. 1 demonstrates a high correlation between the energy and depth for the first 40 craters: the Pearson correlation coefficient is 0.82. At the same time, the nanoablation rate for the subsequent craters weakly correlates with the laser energy (the correlation coefficient is 0.4). Thus, the nanoablation rate is significantly affected by not only the laser energy fluctuations but also the initial lattice state in the irradiated region.

3.2. Influence of the previous laser effect

Along with the lattice inhomogeneity, the nanoablation rate was also found to be significantly affected by the preceding irradiation. In particular, when forming two-dimensional structures with a period of 4 μm, the standard deviation of the crater depth turned out to reach 40%. However, this increase is not related to the stochastic change in etch rate r for different surface points but follows from the fact that the crater depth is systematically smaller in the presence of another crater in the neighborhood.

The following experiment was performed to investigate this effect in more detail. Structures of the same type, consisting of two craters spaced by a distance varied from 3 to 15 μm, were formed by pulsed laser irradiation in the nanoablation regime. Five or six structures were fabricated for each length. A typical surface profile is shown in Fig. 2. The depth of each subsequent crater (spaced by a distance not larger than 8 μm

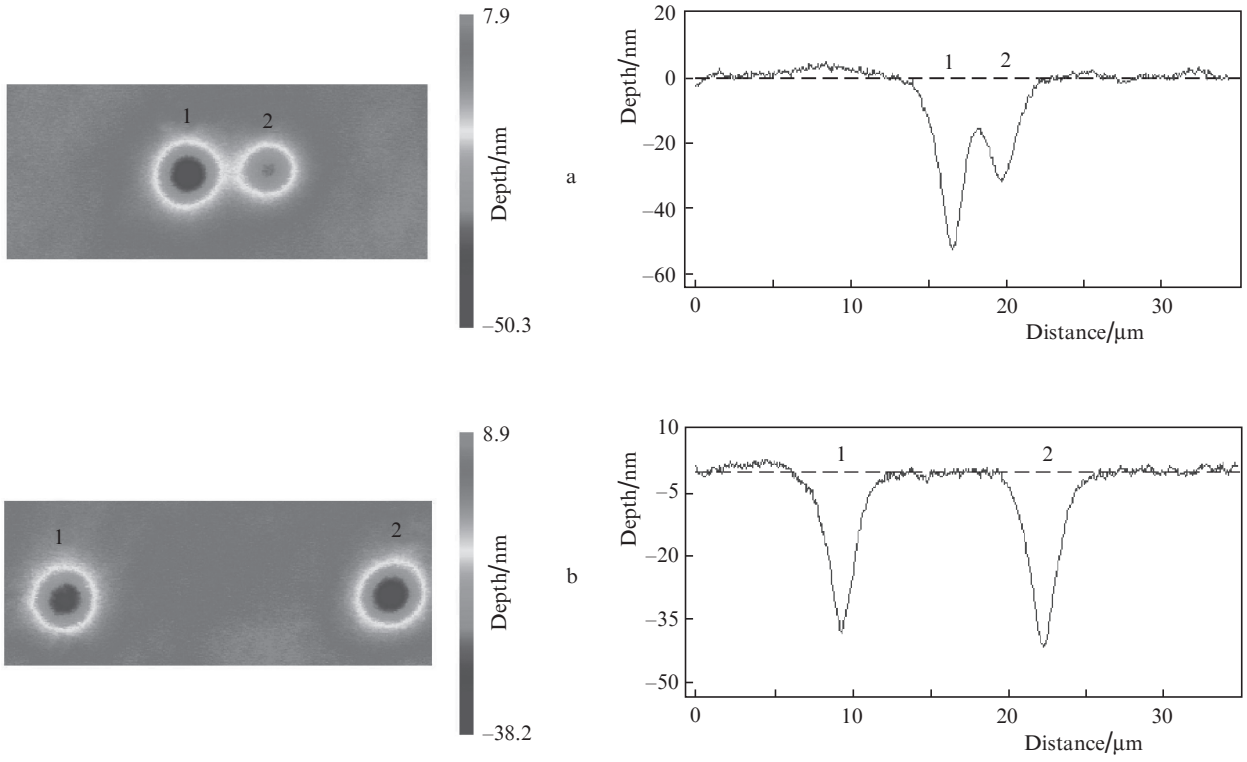

Figure 2. Surface profiles for laser-induced craters on the diamond surface, spaced by (a) 3 and (b) 12 μm.

from the previous one) was always smaller than the previous crater depth.

Figure 3 shows the dependence of the relative difference in the crater depths on the distance between the craters. It can be seen that these data can be separated into two groups. If the length between the craters is less than 8 μm, the depth of the subsequent crater is on average 32% smaller than the depth of the previous one. However, if the distance between the craters exceeds 8 μm, this effect disappears. Note also that the depth fluctuation in each group lies in the same range: 15%.

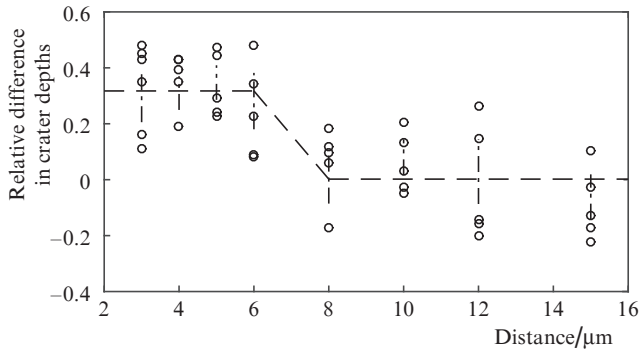

Figure 3. Dependence of the relative difference in the crater depths on the distance between craters.

Thus, it was found that long-term irradiation of the diamond surface by femtosecond pulses not only causes photochemical surface erosion but also forms some permanent change in the neighbourhood, which 'quenches' the lattice, weakening the nanoablation in the next irradiation stage. The mechanism of this effect is not quite clear. Possible factors that can manifest themselves at this characteristic length are the heat diffusion from the irradiated region, the diffusion of defects, and the internal stress.

At first glance, none of these reasons can adequately explain the experimental data. For example, laser heating in principle may lead to the annealing of the diamond lattice and thus reduce the etching rate. However, it is not clear why this process does not affect the etching dynamics in a single spot. Annealing would lead to the etch rate saturation with an increase in the crater depth; nevertheless, the experiment provides close-to-linear dependences.

The most likely explanation of this effect is the deformation (extension) of diamond in the vicinity of the crater. We believe the intermediate stage of nanoablation to be the transformation of the lattice structure at the cluster (or even atomic) level. The experiment performed in [10] showed that, at higher radiation intensities, this transformation leads to the development of conventional ablation in the course of time. In the nanoablation regimes, the transformation rate is lower than the oxidation rate, and changes cannot be accumulated on the surface. Laser irradiation may be accompanied by even slower lattice transformation in the crystal bulk, where oxidation is absent. Accumulation of similar changes in the radiation absorption region forms a domain with a changed density in the caustic and gives rise to a deformation in the surrounding matrix.

3.3. 2D array on the diamond surface and the analysis of its optical properties

The optical properties of the structure formed on the diamond surface were investigated by an example of a two-dimensional (10×10 craters) array with an average depth of

130 nm (Fig. 4). The lattice period was 8 μm (i.e., the effect of 'proximity' was excluded); therefore, the array was 80×80 μm in size. Note that in some compact regions the structure regularity over depth was much higher than that averaged over the sample. For example, the maximum spread in the profile presented in Fig. 4 (with an average depth of 145 nm) is ±5 nm.

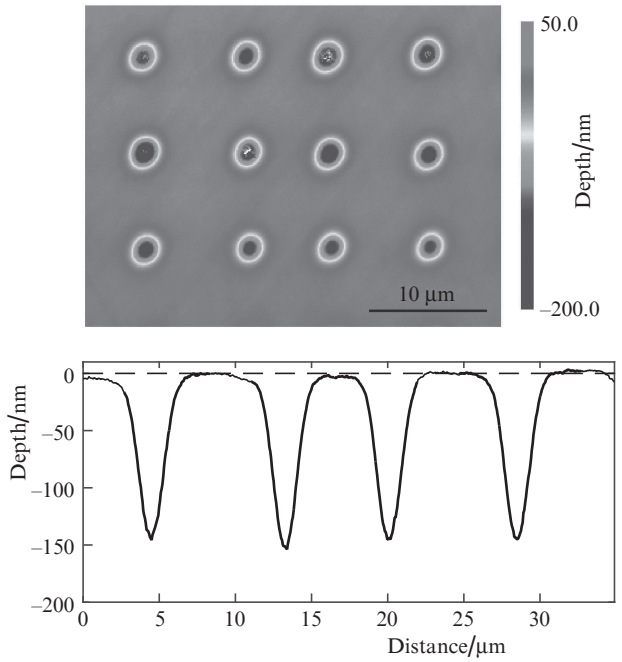

Figure 4. Fragment of a 2D array of craters on the diamond surface.

The optical properties of the structure were analysed using the second harmonic of a cw YAG laser (532 nm), whose beam was focused by a spherical lens with $f = 100$ mm (Fig. 5). A large number of internal inclusions (scattering the probe beam) were observed in the crystal under study. To minimise their influence, we applied the following procedure.

The diffraction analysis system was combined with the laser treatment facility. A diamond sample was moved between the laser treatment and measurement zones using a 150-mm electromechanical movable carriage. First an area free of contaminations and YAG-laser beam distortions was chosen on the sample surface using a microscope (CCD 1). Then a 2D array of craters was formed on this area. After this procedure, the sample was moved again to the probing zone, where the absence of the development of conventional (evaporative) ablation was confirmed (Fig. 5, inset), and then the intensity of the main diffraction maxima was measured [using a movable chamber (CCD 2)] and compared with the calculation results.

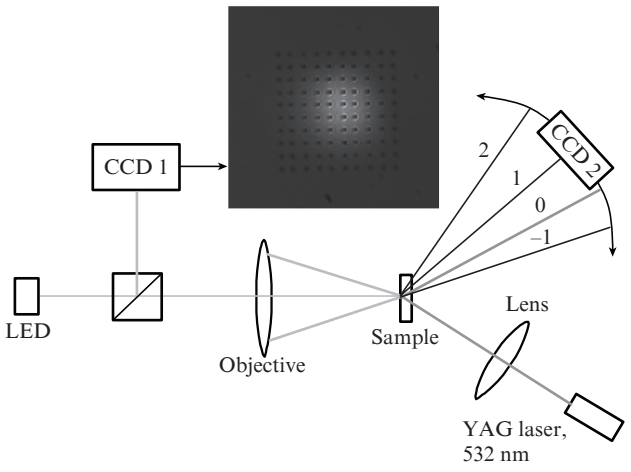

Figure 5. Schematic of the setup for studying the optical properties of nanostructures on the diamond surface.

The diffraction pattern was observed in reflected light. The geometry of the experiment makes it possible to observe 14 main diffraction orders. The others cannot leave the crystal because of the total internal reflection. The sensitivity of the camera in use allowed us to record nine (including zero) diffraction orders.

The diffraction from the grating under consideration was simulated in the GNU Octave environment by numerical calculation of the Fresnel–Kirchhoff integral in the Fraunhofer approximation. The crater profile was assumed to be rectangular with a width of 1.8 μm and a depth equal to the average crater depth (130 nm). The calculation results and the intensity values measured at the center of diffraction orders are presented in Fig. 6. They demonstrate good agreement and show that the 2D array formed on the diamond surface operates as a high-quality phase grating.

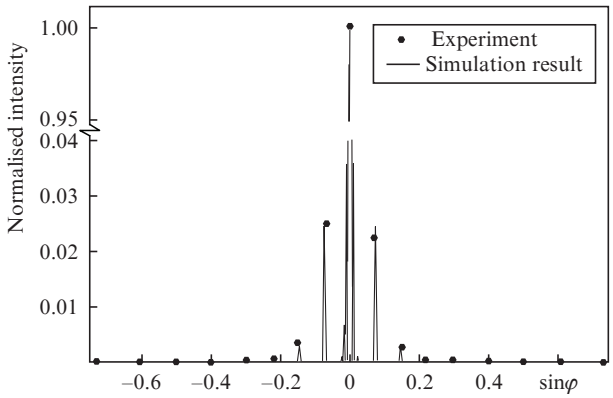

Figure 6. Angular distribution of diffracted light intensity (with zero maximum intensity normalised to unity).

4. Conclusions

It was experimentally shown that laser etching of diamond in the graphitisation-free regime can be used for highly regular nanostructuring of its surface. We investigated the optical properties of one of these structures: an array of 10×10 craters with a base diameter of 4 μm and a depth of 130 nm. The diffraction pattern from this array demonstrated good correspondence between the experimental data and results of numerical simulation. The experimentally estimated regularity of the depth of these structures was shown to be determined by both the fluctuations of laser source energy and the inhomogeneity of the material. A new effect was revealed: the nanoablation rate is significantly (by ~30%) reduced if the irradiated region located at a small (less than 8 μm) distance from the previously irradiated one. This observation is in favour of the concept according to which nanoablation is

accompanied by not only oxidative etching of the surface but also slow accumulative transformation of diamond in the laser beam dissipation zone.

Acknowledgements. This work was supported by the Russian Foundation for Basic Research (Grant No. 14-22-00243).

References

1. Aharonovich L., Greentree A.D., Prawer S. *Nat. Photon*., **5**, 397 (2011).
2. Balmer R.S., Priel I., Woollard S.M., Wort C.J.H., Scarsbrook G.A., Coe S.E., El-Hajj H., Kaiser A., Denisenko A., Kohn E., Isberg J. *Philos. Trans. R. Soc. London, Ser. A*, **366**, 251 (2008).
3. Kononenko V.V., Konov V.I., Pimenov S.M., Prokhorov A.M., Pavel'ev V.S., Soifer V.A. *Kvantovaya Elektron*., **26**, 9 (1999) [*Quantum Electron*., **29**, 9 (1999)].
4. Girolami M., Bellucci A., Calvani P., Cazzaniga C., Rebai M., Rigamonti D., Tardocchi M., Pillon M., Trucchi D.M. *Phys. Status Solidi A*, **212**, 2424 (2015).
5. Konov V. *Laser Photonics Rev*., **6**, 739 (2012).
6. Kononenko V.V., Kononenko T.V., Pimenov S.M., Sinyavskii M.N., Konov V.I., Dausinger F. *Kvantovaya Elektron*., **35**, 252 (2005) [*Quantum Electron*., **35**, 252 (2005)].
7. Khomich A.V., Kononenko V.V., Pimenov S.M., Konov V.I., Gloor S., Luethy W.A., Weber H.P. *Proc. SPIE Int. Soc. Opt. Eng*., **3484**, 166 (1998).
8. Kononenko T.V., Zavedeev E.V., Kononenko V.V., Ashikkalieva K.K., Konov V.I. *Appl. Phys. A*, **119**, 1 (2015).
9. Kononenko V.V., Komlenok M.S., Pimenov S.M., Konov V.I. *Kvantovaya Elektron*., **37**, 1043 (2007) [*Quantum Electron*., **37**, 1043 (2007)].
10. Kononenko V.V., Gololobov V.M., Konov V.I. *Appl. Phys. A*, **122**, 1 (2016).
11. Komlenok M.S., Kononenko V.V., Gololobov V.M., Konov V.I. *Kvantovaya Elektron*., **46**, 125 (2016) [*Quantum Electron*., **46**, 125 (2016)].
12. Kononenko V.V., Gololobov V.M., Komlenok M.S., Konov V.I. *Laser Phys. Lett*., **12**, 096101 (2015).
13. Kononenko V.V., Konov V.I., Gololobov V.M., Zavedeev E.V. *Kvantovaya Elektron*., **44**, 1099 (2014) [*Quantum Electron*., **44**, 1099 (2014)].